



Recent Spin Physics at HERA

D. Ryckbosch^a, on behalf of the HERMES Collaboration

^aDepartment of Subatomic Physics, University of Gent, Belgium

Recent results from the HERMES experiment at HERA are described. The large data set from Run-I has yielded new information on the helicity structure of the nucleon. The data to be taken in Run-II will deal mainly with the transverse spin structure and with exclusive reactions.

1 Introduction

The flavour structure of nucleons is described in terms of Parton Distribution Functions (PDF). The unpolarized PDF $q(x, Q^2)$ gives essentially the probability to find a parton with momentum fraction x in a nucleon. The polarized PDF's describe the spin structure of the nucleon. In particular the longitudinal PDF $\Delta q(x, Q^2)$ gives the helicity distribution of partons in the nucleon. Unpolarized PDF's have been measured in great detail over a wide range in x and Q^2 . The information on polarized PDF's is much more sketchy. A reasonably accurate picture of the quark helicity structure has emerged in recent years, but other aspects of the spin structure remain virtually untouched. Among these the lack of experimental information on the gluon polarization and the transverse spin structure of the nucleon are particularly obvious. Several experiments are gearing up to address these issues in the near future.

This paper reports on some recent results obtained by the HERMES experiment in connection with the longitudinal spin structure of the nucleon, which was the main topic for the HERMES Run-I (1995-2000). The plans for the Run-II (2002-2006+) are discussed in the second half of this contribution. Here the main interest lies in exclusive reactions using a new recoil detector, and the transverse spin structure of the nucleon.

2 The HERMES experiment

HERMES is a fixed target experiment [1] on the 27.6 GeV HERA- e ring. The electrons in the ring are transversely polarized by the Sokolov-Ternov effect, and longitudinal polarization is achieved by a spin rotator in front of the HERMES target. A second rotator behind the experiment restores the transverse polarization. Typical beam polarizations are between 50 and 60%. The polarization of the beam is continuously monitored by two independent Compton backscattering polarimeters.

The beam traverses the HERMES target consisting of a 40 cm long windowless storage cell which confines the injected polarized target gas to the region around the beam. The polarized atomic H and D are provided by an atomic beam source using Stern-Gerlach separation. A small sample of the target gas is continuously analyzed in a Breit-Rabi polarimeter. Typical polarizations are 85%. In 1996 and 1997 data were taken on a polarized proton target, while in 1998, 1999 and 2000 a large data sample was collected on a polarized deuterium target.

The scattered electrons, and some of the hadrons produced in the reaction, are detected in the HERMES spectrometer. This is a typical forward magnetic spectrometer consisting of two symmetric halves above and below the plane of the accelerator. Scattered leptons and produced hadrons are detected and identified within the angular acceptance of ± 170 mrad horizontally and $40 - 140$ mrad vertically. The hadron-lepton separation is done on the basis of the signals in a transition radiation detector, an electromagnetic calorimeter and a pair of scintillator hodoscopes where the second one is preceded by a lead sheet preshower.

The identification of pions, kaons and (anti)protons is performed since 1998 with a Ring Imaging Cherenkov detector (RICH) using clear aerogel and C_4F_{10} gas as radiators [2]. The hadrons can be separated over almost the full momentum range of HERMES, i.e. between 2 and 15 GeV. Before 1998 a threshold Čerenkov was used to give pion identification in a limited momentum range.

The typical kinematic domain for the analysis of polarized DIS in HERMES is $0.1 < Q^2 < 15 \text{ GeV}^2$, $x > 0.02$, with Q^2 the (negative) momentum transfer squared, and $x = Q^2/2M\nu$ the Bjorken scaling variable. To avoid regions with too large contributions of resonance production or radiative corrections further conditions $W > 2 \text{ GeV}$, $y = \nu/E > 0.85$ are usually imposed, with $W^2 = 2M\nu + M^2 - Q^2$ the invariant mass (squared) of the photon-nucleon system and y the fraction of the initial beam energy E transferred.

In semi-inclusive reactions where in addition to the scattered lepton also a produced hadron is detected the fraction of the energy of the virtual photon carried by the hadron is given by $z = E_h/\nu$. To avoid the region with predominantly target fragmentation a cut at $z > 0.2$ is usually used.

3 Inclusive scattering

Most of the information on the PDF's has up to now come from inclusive DIS: experiments where only the scattered lepton is detected. Fig. 1 shows the world data on the polarized structure function $g_1(x)$ for deuterium.

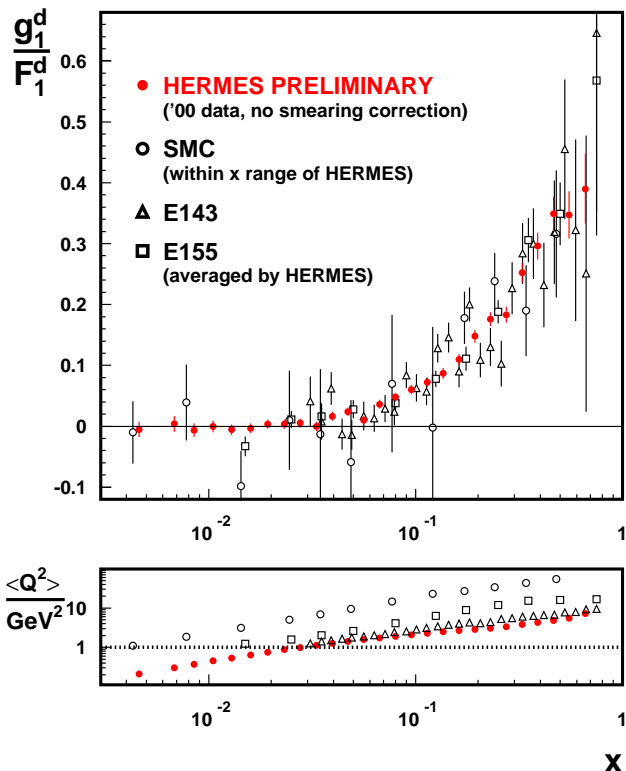


Figure 1. The ratio of the polarized to the unpolarized structure function for deuterium g_1^d/F_1^d . The bottom panel shows the Q^2 values corresponding to each x -bin for the different experiments.

It is obvious from this figure that all experiments are basically in agreement with each other. The recent preliminary HERMES data considerably improve the statistical accuracy. However, there is a difference of about one order of magnitude in the scale of the various experiments, with the SMC results being taken at much higher beam energy than the data from SLAC and HERMES. The fact that the ratio is similar in the different experiments thus implies an evolution for g_1

that is very similar to the one for F_1 . Just as was done successfully in the case of unpolarized structure functions one can analyse the scaling violations observed in $g_1(x, Q^2)$ for proton and neutron targets, and deduce information on the polarization of the different quark flavours and the gluon polarization.

Such a NLO QCD analysis was recently undertaken by HERMES [3]. The results confirm the facts already known about the quark polarization: the quark spin contributes only 20-30% to the spin of the nucleon; most of this contribution comes from the valence quarks; the light quark sea is only little (and negatively) polarized. The gluon polarization that can be derived from the analysis of the presently available data is shown in Fig. 2.

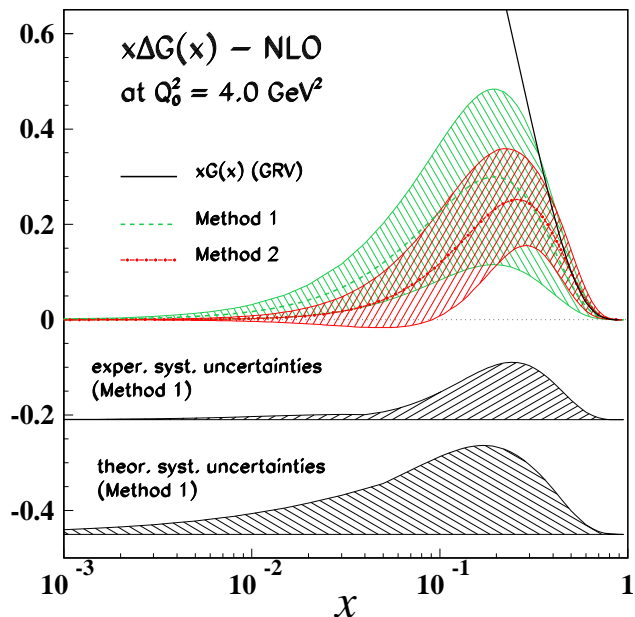


Figure 2. Gluon polarization as derived from a NLO QCD fit to the world data on g_1 [3]. “Method 1” and “Method 2” refer to two different methods to solve the evolution equations. The full line gives the positivity limit.

This figure illustrates that the present data do not really constrain the gluon polarization. The only strong suggestion is that it should be positive, but no value can be given. More direct methods to determine the gluon contribution to the nucleon spin are necessary. This is one of the aims of the COMPASS experiment at CERN which is now starting up. Also the spin physics programme at RHIC intends to determine the gluon polarization independently.

4 Semi-inclusive scattering

4.1 Data and analysis

The HERMES experiment was specifically designed to perform accurate measurements of semi-inclusive reactions, where apart from the scattered lepton also some of the produced hadrons are detected. The idea is that these hadrons contain extra information on the quark that took part in the scattering process. This technique of flavour tagging allows the determination of the polarization of individual quark flavours directly from the spin asymmetries observed in hadron production.

The quantity of interest here is the photon-nucleon asymmetry A_1^h when a hadron of type h is produced, which can be derived from the experimental semi-inclusive spin asymmetry $A_{||}^h$:

$$A_1^h = \frac{A_{||}^h}{D(1 + \eta\gamma)} = \frac{1}{D(1 + \eta\gamma)} \frac{N_h^{\uparrow\downarrow} - N_h^{\uparrow\uparrow}}{N_h^{\uparrow\downarrow} + N_h^{\uparrow\uparrow}} \quad (1)$$

where D is the virtual photon depolarization, η and γ are kinematic factors, and $N_h^{\uparrow\uparrow}$ ($N_h^{\uparrow\downarrow}$) are the number of semi-inclusive events (properly taking into account polarization of target and beam, and relative luminosity) for target polarization parallel (antiparallel) to the beam polarization.

An example of the asymmetries obtained at HERMES is given in Fig. 3. Similar asymmetries were derived for positive and negative pions and on a proton target. A striking feature of the asymmetries in this figure is the fact that the asymmetry for the K^- is compatible with zero. Since this is an all-sea object this already indicates that the polarization of the quark sea will be very small.

In leading order QCD and assuming factorization of the cross section one can write this asymmetry in terms of the PDF and fragmentation functions:

$$A_1^h(x, z) = \frac{\int_{z_m}^1 dz \sum_q e_q^2 \Delta q(x) D_q^h(z)}{\int_{z_m}^1 dz \sum_q e_q^2 q(x) D_q^h(z)} \quad (2)$$

$$= \sum_q P_q^h(x) \frac{\Delta q(x)}{q(x)} \quad (3)$$

In the last equation the *purities* P_q^h are introduced. These are spin-independent quantities which give the probability that a hadron of type h observed in the final state came from a struck quark of flavour q . In that sense they are the inverse of fragmentation functions. The purities depend on the unpolarized quark densities and the fragmentation functions. The former were

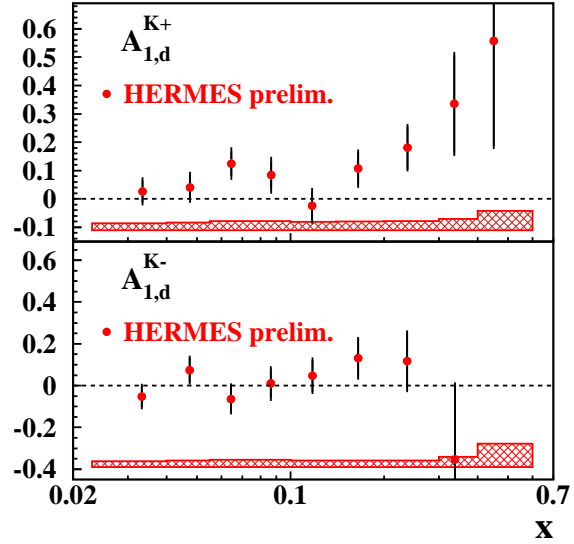


Figure 3. Semi-inclusive spin asymmetries for kaons produced on a deuteron target.

measured to high precision in unpolarized DIS experiments. Information on the fragmentation functions is, however, less precise. There is some information for pions, but those data are taken at quite different kinematics than relevant for HERMES. Hence, the purities were calculated using a Monte Carlo simulation of the entire scattering process. Standard unpolarized parton distribution parametrizations [4] were used, while the fragmentation was modelled in the LUND string model as implemented in JETSET [5]. The LUND model fully describes the fragmentation from the current as well as the target fragmentation region. The parameters of the model were tuned to fit the hadron multiplicities measured at HERMES in order to achieve a good description of the fragmentation process at our kinematics. The resulting purities also include effects of the acceptance of the spectrometer.

The analysis applies Eq. 3 in matrix form:

$$\vec{A}_1(x) = \mathcal{P}(x) \cdot \vec{Q}(x) \quad (4)$$

where the elements of \vec{A}_1 are the measured inclusive and semi-inclusive (Born) asymmetries, the vector \vec{Q} contains the quark (and anti-quark) polarizations and the matrix \mathcal{P} contains as elements the effective integrated purities for the proton and neutron targets. This is an over-constrained system of equations which is solved by a minimisation procedure.

4.2 Results

The purity formalism has been used in the HERMES analysis [6] to make a flavour decomposition

of the quark polarizations for u, \bar{u}, d, \bar{d} , and $s + \bar{s}$. A symmetric strange sea polarization $\Delta s/s = \Delta \bar{s}/\bar{s}$ was assumed. The measured asymmetries were integrated over the z -range from 0.2 to 0.8, and over $Q^2 > 1 \text{ GeV}^2$. The resulting spin densities are shown in Fig. 4.

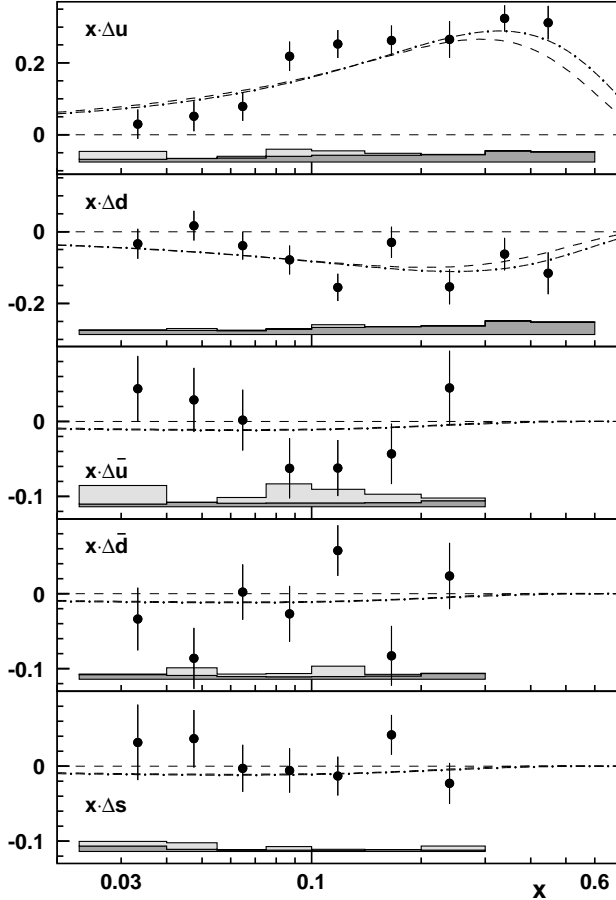


Figure 4. The x -weighted quark spin densities. The dashed line shows a GRSV parameterization [7], and the dash-dotted curve an alternate parameterization due to Blümlein and Böttcher [8].

The polarization of the u -quark is positive over the entire measured range in x , with the largest polarization at high x where the valence quarks dominate. The polarization of the down-quark is negative and also most important in the region of the valence quarks. The polarization of the light sea flavours \bar{u} and \bar{d} , and the polarization of the strange sea are consistent with zero.

The data are compared to polarized PDF's derived from fits to inclusive data. Good agreement is found between the spin densities directly measured here and the results of NLO QCD analyses, in particular for

the valence distributions. The tendency of the parameterizations to yield a negative sea polarization is not confirmed by the data, not is it ruled out with the present statistical accuracy.

The flavour symmetry of the unpolarized light sea is known to be broken. This is experimentally well established through a violation of the Gottfried sum rule. Several models which give a good description of this symmetry breaking in the unpolarized sector also predict a sizeable symmetry breaking in the polarized sector. In particular, most models predict that $\Delta \bar{u} - \Delta \bar{d} > 0$. The flavour asymmetry derived from the present measurement is shown in Fig. 5.

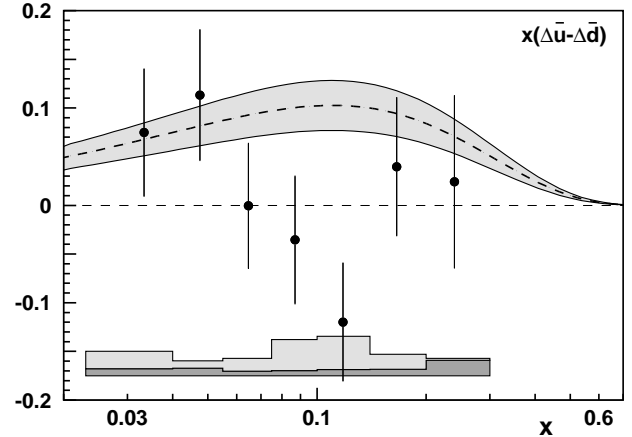


Figure 5. Flavour asymmetry $\Delta \bar{u} - \Delta \bar{d}$ of the light sea extracted from the HERMES purity analysis. The curves show predictions of the Chiral soliton model [9].

The present data do not favour a very strong flavour symmetry breaking. However, the statistical uncertainties are still rather large and further measurements of this quantity will be of great interest.

5 Tensor polarization in deuterium

When analyzing the experimental inclusive spin asymmetries for deuterium in order to deduce the structure function g_1^d one has to take into account a small effect due to possible tensor polarization in this spin 1 target. This is connected with the presence in a spin 1 target of an additional tensor polarized structure function b_1 which relates to the other structure functions F_1 and g_1 as:

$$F_1 = \frac{1}{3} \sum_q e_q^2 (q^+ + q^- + q^0) \quad (5)$$

$$g_1 = \frac{1}{2} \sum_q e_q^2 (q^+ - q^-) \quad (6)$$

$$b_1 = \frac{1}{2} \sum_q e_q^2 [2q^0 - (q^+ + q^-)] \quad (7)$$

where q^+ and q^- denote the probability of finding a quark with helicity parallel to that of the nucleon and q^0 is the probability to find a quark with momentum fraction x in a nucleon with the target in a helicity state 0. b_1 thus measures the difference in parton distributions between a $m = 1$ and a $m = 0$ target.

The HERMES target is capable of producing highly tensor polarized deuterium. This was done during a short run in 2000 with an average polarization of 83%. The tensor polarized structure function can be found from the experimental tensor asymmetry:

$$A_T = \frac{(\sigma^+ + \sigma^-) - 2\sigma^0}{\sigma^+ + \sigma^- + \sigma^0} \propto -\frac{2}{3} \frac{b_1}{F_1} \quad (8)$$

The preliminary HERMES result for this asymmetry is shown in Fig. 6, while the deduced tensor structure function b_2 (trivially related to b_1 through: $b_2 = 2x(1+R)b_1/(1+\gamma^2)$) is shown in Fig. 7. The

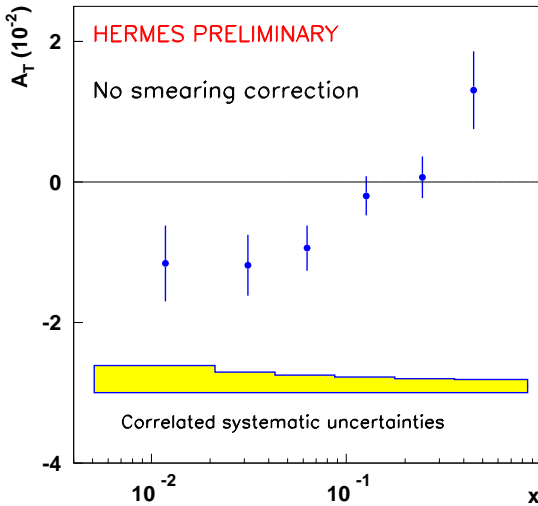


Figure 6. Tensor asymmetry for deuterium.

small values found for the tensor asymmetry (of the order 1%) show that the effect on the determination of the helicity structure function g_1 can safely be neglected. The actual tensor structure function b_2^d is significantly different from zero, in particular at lower values of x . It is in broad agreement with the model calculations of Ref. [10].

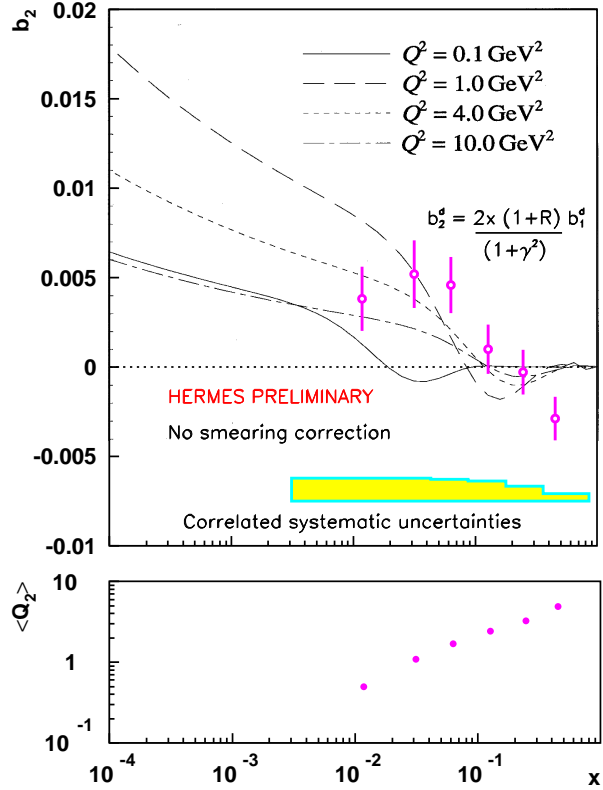


Figure 7. Tensor structure function b_2^d . The lines show the predictions of Ref. [10] for different values of Q^2 .

6 Exclusive reactions

Exclusive DIS reactions, where the target nucleon remains in or close to its ground state, can be described in terms of the Generalized Parton Distributions (GPD) that were introduced a few years ago. These GPD's form a natural off-forward extension of the standard Parton Distribution Functions which are well determined from (semi-)inclusive DIS reactions. They form a connection between the PDF's and the form-factors of hadrons.

The cleanest example of the appearance of GPD's in an exclusive reaction is that of Deeply Virtual Compton Scattering (DVCS). The main diagram for this reaction is shown in Fig. 8. There are 4 (flavour sets of) GPD's: 2 unpolarized functions (H and E) and 2 polarized (\tilde{H} and \tilde{E}). The two functions E and \tilde{E} correspond to helicity flip operators and have no direct analogon in the forward PDF's. The functions H and \tilde{H} have as their forward limit the standard unpolarized and polarized PDF's F_1 and g_1 , respectively. The GPD's depend on 3 independent kinematic variables: $H(x, \xi, t)$ where ξ is related to the usual Bjorken variable by $2\xi = \frac{x_B}{1-x_B/2}$. (Note that there are other equivalent choices possible for the variables.)

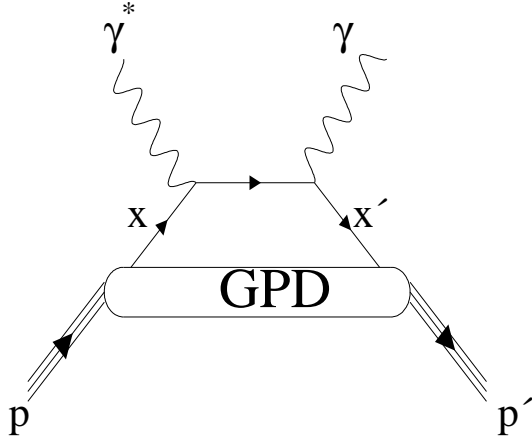


Figure 8. Handbag diagram describing DVCS.

The importance of GPD's in the context of spin physics is embodied by the sum rule which was derived by Ji [11] for the second moment of the GPD's:

$$\frac{1}{2} \int_{-1}^{+1} x [H^q(x, \xi, t=0) + E^q(x, \xi, t=0)] dx = J_q \quad (9)$$

where J_q is the *total* angular momentum contribution of quarks to the spin of the nucleon. Up to now there is experimental information only on the contribution from the spins of quarks (and gluons). Combined with this sum rule GPD's and thus exclusive reactions are the only way presently known that may lead to information on the orbital angular momentum contribution, thus providing a complete picture of the nucleon spin structure.

The main problem in the experimental determination of the GPD's is the fact that they do not appear as simple factors in the expressions for cross sections, asymmetries etc. They always appear in convolutions over the x and ξ variables, making a direct determination impossible. Finding the best deconvolution procedure to lead from the experimental data to the GPD is a challenge for the future. To do this a good understanding of the structure of the GPD is essential to develop adequate models.

Fig. 9 shows the missing mass (squared) spectrum for the DVCS reaction at HERMES. A clear peak at the ground state mass can be seen, thus establishing the observation of exclusive DVCS. However, at the HERMES kinematics with relatively low beam energy the main source of hard photons is not DVCS but the

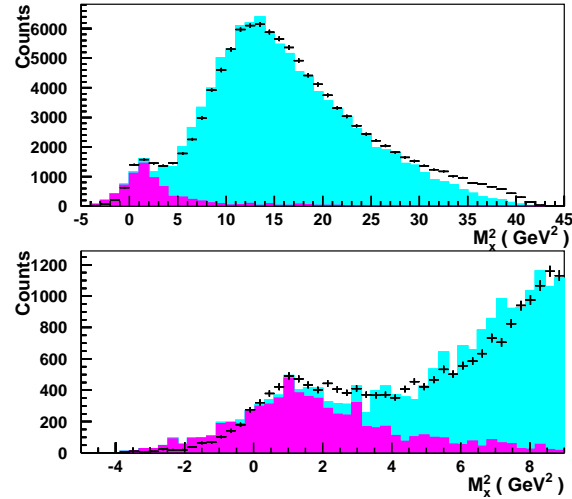


Figure 9. Missing mass distribution for electroproduction of real photons [12]. The dark histogram shows the simulated contribution of exclusive photon production, while the light histogram corresponds to photons produced in fragmentation processes (mainly π^0 production).

Bethe-Heitler process where the photon is radiated from either the incoming or the outgoing electron. It is in principle impossible to disentangle these two processes. On the other hand the presence of two processes will also lead to interference between them and this can be exploited to access the DVCS amplitude. The interference terms can be projected out by measuring azimuthal asymmetries in single photon electroproduction. It was shown [13] that beam-spin (A_{LU}), target-spin (A_{UL}) and beam-charge (A_C) azimuthal asymmetries provide access to different combinations of the real and imaginary parts of the interfering amplitudes. It should be noted that at present HERA is the only place where beam charge asymmetries can be studied because of the availability of both electron and positron beams.

In Fig. 10 the beam-spin azimuthal asymmetry for a proton target is shown, while Fig. 11 presents the results for the beam-charge asymmetry on the proton. The $\sin \phi$ moment of the former one is related to the imaginary part of the interference amplitude; the $\cos \phi$ moment of the latter is related to the real part of the interference amplitude. It is obvious from the results presented in these figures that the DVCS-BH interference indeed dominates the distributions. The extracted $\sin \phi$ and $\cos \phi$ moments are in encouraging agreement with theoretical calculations based on models of GPD's. In a next step the kinematic distributions of the various moments of the azimuthal asym-

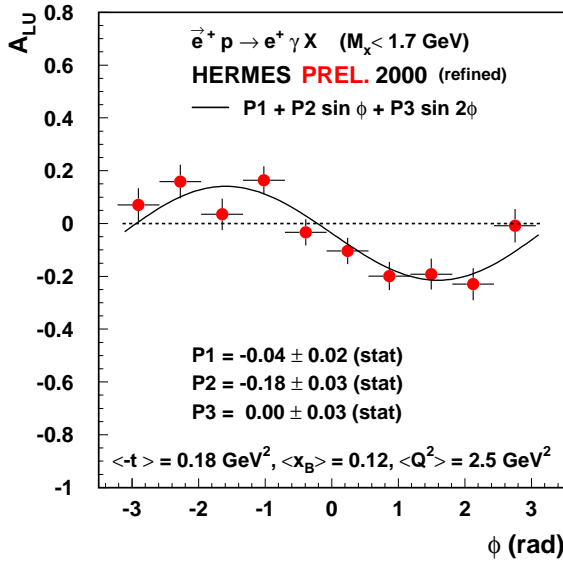


Figure 10. The beam-spin azimuthal asymmetry for exclusive real photon production on a hydrogen target.

metries are extracted and to be compared to more detailed calculations.

From Fig. 9 it can be seen that the experimental resolution of the HERMES spectrometer is insufficient to allow a clear separation of exclusive and fragmentation processes. At present only the scattered electron and the real photon are detected in the forward spectrometer. To really establish exclusivity on the event level would require the detection of the recoil target proton. Kinematics dictate that this proton recoils with low momentum at high angles relative to the beam line, outside the present acceptance of the HERMES spectrometer. A major project at HERMES now is the construction of a recoil detector to detect and identify such recoil particles. The detector will consist of three active detector parts. A silicon detector around the target cell inside the beam vacuum, a scintillating fibre tracker in a longitudinal magnetic field and a layer of scintillator strips with interspersed W-sheets as preshower material.

It is planned to install the recoil detector somewhere in 2004 or 2005 and to operate it for on the order of 2 years with an unpolarized hydrogen target and polarized electron and positron beams. The higher target densities that are possible for unpolarized targets will enable HERMES to obtain a large data sample on DVCS with unprecedented statistical and systematic accuracy for both beam-spin and beam-charge asymmetries. An added advantage of the recoil detector is that the determination of the momentum of the recoil proton immediately yields an accurate measurement of

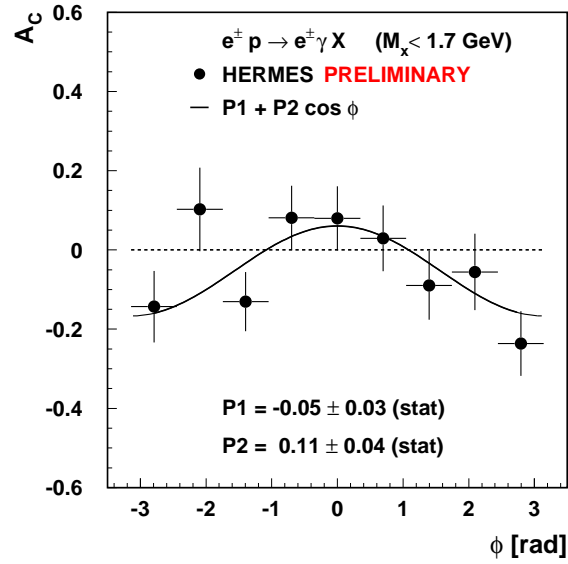


Figure 11. The beam-charge azimuthal asymmetry for exclusive real photon production on a hydrogen target.

the momentum transfer $-t$ to the target. This will improve the resolution in this important kinematic quantity (see e.g. Eq. 9) by about an order of magnitude.

7 Transversity

Up to now we have only discussed the helicity structure of the nucleon. In fact there are three different structure functions which describe the parton structure of the nucleon at leading twist. These are the unpolarized structure function F_1 , the helicity structure function g_1 and a new quantity, transversity h_1 . The related PDF is denoted $h_1^q(x)$ and gives the probability to find a transversely polarized quark in a transversely polarized nucleon. It is experimentally unknown, mainly because as a chiral-odd object it cannot be measured through inclusive DIS. In combination with another chiral-odd object, e.g. a fragmentation function, transversity becomes accessible. In semi-inclusive reactions it leads to single-spin azimuthal asymmetries in e.g. pion and kaon production on a transversely polarized target.

Such a transversely polarized target is installed in HERMES since 2001. First data have been taken with it after HERA became operational again following a major luminosity upgrade for the collider experiments. However, at the present time the collected data sample is too small to make a measurement of the transversity distributions feasible. This will come in the run of 2003 and 2004. On the other hand, HERMES has already collected a large amount of data on a longi-

tudinally polarized target. Such a target is longitudinal with respect to the incoming electron beam, but does contain a small ($\approx 10 - 15\%$) transverse component with respect to the virtual photon. Moreover, there is a number of higher-twist distribution functions and fragmentation functions which are directly related to the transversity distribution and which also cause single-spin asymmetries in semi-inclusive reactions on a longitudinal target.

The experimental single-spin azimuthal asymmetry for positive and negative pions on a longitudinally polarized proton target is depicted in Fig. 12. The positive pions show a clear $\sin \phi$ modulation of the asymmetry, while this is absent for negative pions. This is consistent with the picture of u -quark dominance. A larger set of results on such asymmetries for a deuteron target was recently published [14]. Theoretical calculations based on models of the transversity distribution have had some success in reproducing these data.

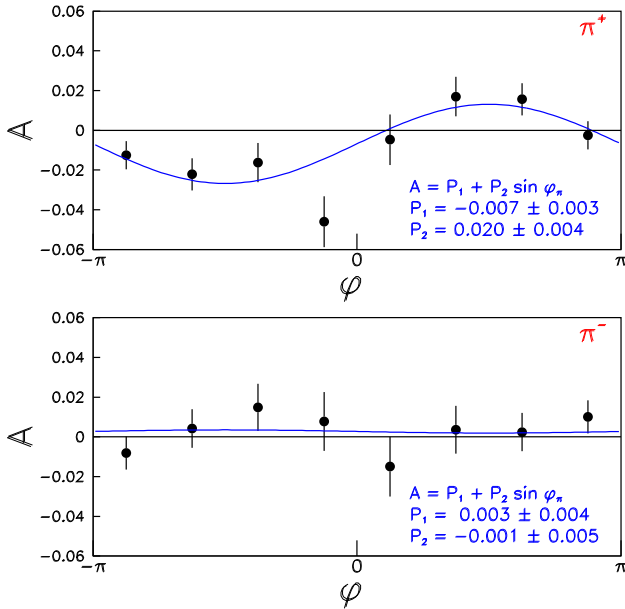


Figure 12. ϕ -dependence of the single-spin azimuthal asymmetry in semi-inclusive pion production on a longitudinally polarized proton target.

8 Conclusions

Some recent results from the HERMES experiment at HERA were presented. The analysis of the large data set on longitudinally polarized proton and deuteron targets, collected in the first run of HERMES from 1995 through 2000, is nearing completion. Results of a NLO QCD analysis of the inclusive scattering show

indications for a positive and possibly large gluon polarization. The results from the semi-inclusive analysis are consistent with those from the inclusive data and moreover give for the first time a flavour decomposition of the quark polarizations in 5 components. The valence quarks are seen to dominate the contribution of the quark spins to the nucleon spin, while the sea appears to have a negligible polarization.

The observation of azimuthal asymmetries in exclusive reactions, here exemplified by the DVCS reaction, promises access to the new GPD's. The implementation of the recoil detector now under construction at HERMES will give a much enhanced accuracy for such studies.

The main thrust of the data taking of HERMES at the present time is with a transversely polarized proton target. On the basis of single-spin azimuthal asymmetries observed in semi-inclusive scattering off a longitudinally polarized target it can be expected that these data will give first experimental information on the transversity distribution of quarks in the nucleon.

References

1. K. Ackerstaff *et al.* [HERMES Collaboration], Nucl. Instr. Meth. A **417** (1998) 230.
2. A. Akopov *et al.*, Nucl. Instr. Meth. A **479** (2002) 511.
3. L. De Nardo, Dissertation, University of Alberta (2002)
4. H. Lai *et al.*, Eur. Phys. J. C **12** (2000) 375.
5. T. Sjostrand, Comp. Phys. Comm. **82** (1994) 74.
6. A. Airapetian *et al.* [HERMES Collaboration], hep-ex/0307064.
7. M. Glück, E. Reya, M. Stratmann, and W. Vogelsang, Phys. Rev. D **63** (2001) 094005.
8. J. Blümlein and H. Böttcher, Nucl. Phys. B **636** (2002) 225.
9. B. Dressler *et al.*, Eur. Phys. J. C **14** (2000) 147.
10. K. Bora and R. L. Jaffe, Phys. Rev. D **57** (1998) 6906.
11. X. Ji, Phys. Rev. Lett. **78** (1997) 610.
12. A. Airapetian *et al.* [HERMES Collaboration], Phys. Rev. Lett. **87** (2001) 182001.
13. M. Diehl *et al.*, Phys. Lett. B **411** (1997) 192.
14. A. V. Belitsky *et al.*, Nucl. Phys. B **629** (2002) 323.
15. A. Airapetian *et al.* [HERMES Collaboration], Phys. Lett. B **562** (2003) 182.